



Published in final edited form as:

ACS Nano. 2009 March 24; 3(3): . doi:10.1021/nn900188t.

Micro-Mirrors for Nanoscale Three-Dimensional Microscopy

Kevin Seale[†], Chris Janetopoulos[‡], and John Wikswo^{†,§,*}

[†]Department of Biomedical Engineering, Vanderbilt University, Nashville, Tennessee 37235-1807

[‡]Department of Biological Sciences, Vanderbilt University, Nashville, Tennessee 37235-1807

[§]Departments of Molecular Physiology & Biophysics and Physics & Astronomy, Vanderbilt University, Nashville, Tennessee 37235-1807

Abstract

A research-grade optical microscope is capable of resolving fine structures in two-dimensional images. However, three-dimensional resolution, or the ability of the microscope to distinguish between objects lying above or below the focal plane from in-focus objects, is not nearly as good as in-plane resolution. In this issue of *ACS Nano*, McMahon *et al.* report the use of mirrored pyramidal wells with a conventional microscope for rapid, 3D localization and tracking of nanoparticles. Mirrors have been used in microscopy before, but recent work with MPWs is unique because it enables the rapid determination of the x -, y -, and z -position of freely diffusing nanoparticles and cellular nanostructures with unprecedented speed and spatial accuracy. As inexpensive tools for 3D visualization, mirrored pyramidal wells may prove to be invaluable aids in nanotechnology and engineering of nanomaterials.

Before the development of the modern research microscope, scientists had only rudimentary magnifying tools to observe microscopic structures. This inevitably led to some ideas about microscopic life that seem unusual today, including the proposition that humans sprout from a homunculus, a tiny man scrunched up inside the head of a sperm cell (depicted in Figure 1). After more than 300 years of development, the microscope now allows us to see the previously unseen world with pictures that are becoming clearer every day. A research-grade optical microscope is now capable of resolving structures 200 nm apart—easily small enough to disprove the homunculus hypothesis! However, the z -axis resolution, or the ability of the microscope to distinguish between objects lying above or below the focal plane from in-focus objects, is not nearly as good as the in-plane resolution. In this issue of *ACS Nano*, McMahon *et al.*¹ report the use of mirrored pyramidal wells (MPWs) with a conventional microscope for rapid, three-dimensional (3D) localization and tracking of nanoparticles. Mirrors, including silicon pyramidal wells²⁻⁴ and other techniques for 3D microscopy and particle localization, such as scanning near-field microscopy,⁵⁻⁹ have been used before.¹⁰⁻²⁴ Recent work with mirrored pyramidal wells is unique because it enables the rapid determination of the x -, y -, and z -position of freely diffusing nanoparticles and cellular nanostructures with unprecedented speed and spatial accuracy. The point localization algorithm reported by McMahon *et al.*¹ is very fast using MPWs because it finds the center of mass of the primary and reflected diffraction patterns without having to focus the microscope and, for a point source, even provides spatial localization better than historically described limits of microscopy such as the Abbe limit or Rayleigh criterion.²⁵

Fabrication of Mirrored Pyramidal Wells

The mirrors are made by wet etching single-crystalline silicon wafers with a caustic such as potassium hydroxide. An overview of the process is available in several texts,²⁶ and specific MPW protocols and references can be found elsewhere.² The $\langle 111 \rangle$ crystal plane etches much slower than the other planes, which causes anisotropic removal of silicon, resulting in four-sided pyramid-shaped wells. The size and location of the base of the pyramid are specified by a mask, and the peak may be pointed or flattened depending on the etch time. The walls are then coated with a reflective material such as aluminum, gold, or platinum and form excellent mirrors. Other crystals such as sapphire or quartz may also be used with similar processes to produce smooth angled surfaces,^{27,28} and replica molding can be used to transfer the pattern to other materials. The silicon wells are introverted, meaning that the angle of the walls is steeper than 45° . This requires that the sample be physically placed inside the well to obtain simultaneous images. The silicon wells can be advantageous for trapping particles for imaging and/or chemical reactions but also introduce some challenges. Samples cannot be trans-illuminated because the wafer is opaque, and it may be difficult to hold a sample in a MPW if one uses an inverted (rather than upright) microscope.

We have developed other methods of making MPWs, including direct embossing of clear plastics and metallic aluminum to produce *extroverted* wells with wall angles that are less than 45° . Figure 2 illustrates a seven-perspective simultaneous image of an autofluorescent *Helianthus annuus* pollen grain using an extroverted well with wall angles of 35.3° (the exact inverse of our silicon wells). The pollen grain is resting on a coverslip with the MPW positioned just above it. Extroverted wells are more useful for samples that cannot be easily placed inside an introverted well. For instance, we have used extroverted wells to image cells and other specimens resting on a coverslip on an inverted microscope platform. The ability to control the angle of the mirrors is a great advantage. Perfectly orthogonal vantage points with a mirror angle of 45° would resolve 3D motion unambiguously into x -, y -, and z -components—something that could be achieved with a ground and polished embossing tool but not Si etching.

Interpreting the Image: 3D versus 2D Microscopy

Although microscopy has become commonplace, there is a hidden complexity in the representation of a 3D specimen as a two-dimensional (2D) image that can lead to serious misconceptions, especially with 3D microscopy. The physics of light diffraction and point spread function (PSF) of the microscope objective underlie the inherent limitation of the ability of the microscope to discriminate between objects at different distances from the front aperture. As illustrated in the schematic in Figure 3, the PSF is the complex, 3D intensity distribution on the image side of a lens or objective that arises when a perfect point source of light lies in the focal plane on the object side. In comparison with an ideal imaging apparatus in which a point source of light would be represented as intensity at a single point in space on the image side, a real objective spreads the intensity over a small volume. The shape of the PSF naturally depends on the shape, size, and position of the lenses or diffracting elements of the objective but is theoretically a complex arrangement of intensity minima and maxima that are radially symmetric about the optical axis and roughly bilaterally symmetric about the focal plane^{25,29} for linear shift-invariant optical systems. For modern research microscope objectives with high numerical apertures, the central maxima of the PSF is typically ~ 200 nm wide and can be much larger in the z -direction, depending on the objective. Higher-order maxima occur at radial positions that depend on the distance from the focal plane and appear in the image as rings of light surrounding the point source (Figure 4). Unless the specimen is a point source, the asymmetric central and higher-order maxima confound the determination of the 3D object location or structure.

Recent work with mirrored pyramidal wells is unique because it enables the rapid determination of the x -, y -, and z -position of freely diffusing nanoparticles and cellular nanostructures with unprecedented speed and spatial accuracy.

While the demonstration of nanoparticle localization is important, scientists typically do not study isolated point sources with a microscope, but rather optically complex 3D objects such as cells and tissues. Mathematically, image formation by a microscope involves convolution. The object is represented as a 3D arrangement of single point sources (light scattering centers or emitters such as fluorescent proteins), and a single image is a planar slice through the 3D intensity distribution represented by the convolution of the PSF with the object. A 3D image set, or cube, is an assembly of images collected at precise intervals of focal depth, which, when taken together, span the entire specimen. Recovery of the actual object from the image data requires that the PSF be deconvolved from the 3D image cube. For mathematical and computational reasons, convolution and de-convolution are more easily accomplished in the spatial frequency domain using the Fourier-transformed images and PSF. The Fourier transform of the PSF is somewhat doughnut-shaped with a conspicuous cone-shaped swath of missing spatial frequencies along the z -direction. Three-dimensional microscopy has long suffered from the missing cone of frequencies in the Fourier transform of the PSF, and many sophisticated methods for overcoming this limitation have been devised.²⁵ Perhaps the most significant advantage of MPWs is also the simplest. By reflecting the side view of the sample into the xy plane, the MPWs allow direct inspection of z features that are normally masked by the missing cone problem; for instance, the 3D trajectory of the microtubule organizing center and other cytosolic features of a motile cell.²

Scientists have tried overcoming the limitation of the missing cone of frequencies to find out what cells look like in three dimensions in various ways: laying microscopes sideways, creating large mirrored chambers, combining multiple orthogonal objectives, sandwiching the sample between objectives, and more mathematically sophisticated approaches of optical sectioning microscopy with 3D reconstruction on both wide-field and confocal microscope platforms.^{30,31} The effect of the missing cone can be visualized by imagining an infinitely thin, infinitely large plane of featureless fluorescent film near the focal plane of a microscope, such as a perfectly smooth, dye-coated coverslip. The observer looking through the binoculars can adjust the focus knob in any direction without ever gaining a sense of the plane's distance from the objective. In-plane features with high spatial frequencies, such as dust specks, scratches, or cells, which the typical microscopists take for granted, are actually required to "home in" on the focal plane. With an actual microscope specimen such as a cell, out-of-focus features can contribute to the image in unwanted ways that cannot be known or corrected. The MPWs attack this problem head on with simultaneous flanking views of the specimen that reveal much about its overall spatial distribution. If the microscope is carefully aligned with the MPW, simple matrix transformations on image features can be used to generate 3D data from the reflected images. Figure 5 illustrates a budding yeast cell in a MPW and a 3D plot of the transformed perimeter points of the reflections.

Another important advantage provided by the mirrored wells is a dramatic increase in the collection efficiency (CE), a measure of the light-gathering ability of an imaging system. When using a simple objective, the collection efficiency is synonymous with the numerical aperture (NA) of the objective, with a higher NA implying a greater CE for a given media refractive index. Although light sources or light scattering centers produce light traveling in all directions, only the photons having trajectories aligned with the collection cone of the objective are collected. The higher NA objectives typically have collection cones with half angles greater than 60° and very short working distances to gather as much of the sample light as possible. With the use of mirrored wells, the CE and NA are uncoupled, and inexpensive objectives with relatively low NA and longer working distances can have a

significantly higher CE than very expensive, high NA objectives. This is because more of the available light is redirected by specular reflection into the collection cone of the objective.

The ability to micromachine and mass fabricate the mirrored wells makes them attractive to researchers in many fields of science. Hajjoul *et al.* have incorporated mirrored channels into MEMS devices for studying individual yeast cells,⁹ and our group has coupled mirrored wells to a multitrapp nanophysiometer.³² The pyramidal wells have been used by other researchers to trap atoms with lasers⁸ and as microbeakers that contain bead-based chemical reactions for protein detection.^{33,34} Mirrored pyramidal wells that are etched through the wafer offer additional opportunities for microfluidic flow applications and trans-illumination.

Just as Nicholas Hartsoecker and his colleagues pioneered the use of magnifying optics to observe microscopic life, so today's nano-technology researchers are breaking through barriers to observe and to engineer material at the subcellular scale. As researchers begin to engineer functional nanostructures and to integrate them with larger assemblies, it becomes increasingly important for light microscope technology to provide accurate 3D information. This is perhaps especially true in bionanotechnology, where the nanostructures may be seamlessly integrated with naturally occurring structures such as proteins, nucleic acids, or other small molecules within the milieu of a living cell. For example, aggregation of functionalized quantum dots for rapid and sensitive biomarker detection would benefit from 3D microscopy with submicron resolution in all three spatial dimensions.^{35,36} Fueled by discoveries stemming from the genomic revolution, the cell, the basic unit of life, is gaining unprecedented significance in the context of human society. As engineered cells become a mainstay of many large industries, including agriculture, pharmaceuticals, biofuels, and bioremediation, biointegrated nanostructures for actuation and detection or as end products will grow more important.³⁷ As science enters the nanotechnology age, compact, inexpensive technology such as MPWs (Figure 6) for precise 3D localization and control at the nanometer scale will be invaluable aids.

As researchers begin to engineer functional nanostructures and integrate them with larger assemblies, it becomes increasingly important for light microscope technology to provide accurate 3D information.

Acknowledgments

The authors wish to acknowledge helpful conversations with Sanford Simon, Mats Gustafsson, Carol Cogswell, Thomas Brown, and Chrysan-the Preza, and editorial and bibliographic assistance of Allison Price and Don Berry.

REFERENCES AND NOTES

1. McMahon MD, Berglund AJ, Carmichael P, McClelland JJ, Liddle AJ. 3D Particle Trajectories Observed by Orthogonal Tracking Microscopy. *ACS Nano*. 2009; 3:609–614. [PubMed: 19309171]
2. Seale KT, Reiserer RS, Markov DA, Ges IA, Wright C, Janetopoulos CJ, Wikswo JP. Mirrored Pyramidal Wells for Simultaneous Multiple Vantage Point Microscopy. *J. Microsc.* 2008; 232:1–6. [PubMed: 19017196]
3. Seale, KT.; Reiserer, RS.; Markov, D.; Ges, I.; Wikswo, JP. BioMEMS Micromirror Wells for High Resolution Simultaneous Three Dimensional Imaging of Cells. 2006 Annual Fall Meeting of the Biomedical Engineering Society; October 11–14, 2006; Biomedical Engineering Society; p. 1238
4. Seale, KT.; Reiserer, RS.; Markov, D.; Ges, I.; Janetopoulos, C.; Wikswo, JP. Focus on Microscopy International Symposium. Valencia; Spain: Apr 10–13. 2007 Simultaneous Multiperspective Three Dimensional Microscopy with Mirrored Pyramidal Wells.

5. Betzig E, Finn PL, Weiner JS. Combined Shear Force and Near-Field Scanning Optical Microscopy. *Appl. Phys. Lett.* 1992; 60:2484–2486.
6. Betzig E, Trautman JK. Near-Field Optics: Microscopy, Spectroscopy, and Surface Modification Beyond the Diffraction Limit. *Science.* 1992; 257:189–195. [PubMed: 17794749]
7. Betzig E, Chichester RJ. Single Molecules Observed by Near-Field Scanning Optical Microscopy. *Science.* 1993; 262:1422–1426. [PubMed: 17736823]
8. Trupke M, Ramirez-Martinez F, Curtis EA, Ashmore JP, Eriksson S, Hinds EA, Moktadir Z, Gollasch C, Kraft M, Prakash GV, et al. Pyramidal Micromirrors for Microsystems and Atom Chips. *Appl. Phys. Lett.* 2006; 88:071116-1–071116-3.
9. Hajjoul, H.; Girard, J.; Dilhan, M.; Kocanova, S.; Bystricky, K.; Bancaud, A. Novel Approach for 3D Live Cell Fluorescence Microscopy Based on Microfabricated Mirrors. The 12th International Conference on Miniaturized Systems for Chemistry and Life Sciences; October 12–16, 2008; Chemical and Biological Microsystems Society; p. 1B3
10. Gustafsson MGL, Agard DA, Sedat JW. 15M: 3D Widefield Light Microscopy with Better Than 100 nm Axial Resolution. *J. Microsc.* 1999; 195:10–16. [PubMed: 10444297]
11. Bell L, Jeon K. Locomotion of Amoeba Proteus. *Nature.* 1963; 198:675–676.
12. Gustafsson T, Wolpert L. Cellular Movement and Contact in Sea Urchin Morphogenesis. *Biol. Rev.* 1967; 42:442–498. [PubMed: 4864367]
13. Boocock CA, Brown AF, Dunn GA. A Simple Chamber for Observing Microscopic Specimens in Both Top and Side Views. *J. Microsc.* 1985; 137:29–34. [PubMed: 3973917]
14. Cao J, Usami S, Dong C. Development of a Side-View Chamber for Studying Cell-Surface Adhesion under Flow Conditions. *Ann. Biomed. Eng.* 1997; 25:573–580. [PubMed: 9146810]
15. Dong C, Cao J, Struble EJ, Lipowsky HW. Mechanics of Leukocyte Deformation and Adhesion to Endothelium in Shear Flow. *Ann. Biomed. Eng.* 1999; 27:298–312. [PubMed: 10374723]
16. Leyton-Mange J, Yang S, Hoskins MH, Kunz RF, Zahn JD, Dong C. Design of a Side-View Particle Imaging Velocimetry Flow System for Cell-Substrate Adhesion Studies. *J. Biomech. Eng.* 2006; 128:271–278. [PubMed: 16524340]
17. Harris A. Initiation and Propagation of Ruffle in Fibroblast Locomotion. *J. Cell Biol.* 1969; 43:165A–166A.
18. Hlinka J, Sanders FK. Real and Reflected Images of Cells in Profile. I. A Method for Study of Cell Movement and Adhesion. *J. Cell Sci.* 1972; 11:221–231. [PubMed: 4561136]
19. Ingram VM. A Side View of Moving Fibroblasts. *Nature.* 1969; 222:641–644. [PubMed: 5768273]
20. Roth KE, Rieder CL, Bowser SS. Flexible-Substratum Technique for Viewing Cells From the Side: Some *in vivo* Properties of Primary (9 + 0) Cilia in Cultured Kidney Epithelia. *J. Cell Sci.* 1988; 89:457–466. [PubMed: 3058727]
21. Sanders EJ, Prasad S. Observation of Cultured Embryonic Epithelial-Cells in Side View. *J. Cell Sci.* 1979; 38:305–314. [PubMed: 391813]
22. Lindek S, Stefany T, Stelzer EHK. Single-Lens Theta Microscopy—A New Implementation of Confocal Theta Microscopy. *J. Microsc.* 1997; 188:280–284.
23. Lindek S, Swoger J, Stelzer EHK. Single-Lens Theta Microscopy: Resolution, Efficiency and Working Distance. *J. Mod. Opt.* 1999; 46:843–858.
24. Sheppard CJR. Fundamental Reduction of the Observation Volume in Far-Field Light-Microscopy by Detection Orthogonal to the Illumination Axis: Confocal Theta-Microscopy. *Opt. Commun.* 1995; 119:693–695.
25. Heintzmann R, Ficz G. Breaking the Resolution Limit in Light Microscopy. *Briefings Funct. Genomics Proteomics.* 2006; 5:289–301.
26. Madou, MJ. Fundamentals of Microfabrication: The Science of Miniaturization. CRC Press; Boca Raton, FL: 2002.
27. Wang J, Guo LW, Jia HQ, Wang Y, Xing ZG, Li W, Chen H, Zhou JM. Fabrication of Patterned Sapphire Substrate by Wet Chemical Etching for Maskless Lateral Overgrowth of GaN. *J. Electrochem. Soc.* 2006; 153:C182–C185.
28. Hedlund C, Lindberg U, Bucht U, Soderkvist J. Anisotropic Etching of Z-Cut Quartz. *J. Micromech. Microeng.* 1993; 3:65–73.

29. Born, M.; Wolf, E. Principles of Optics. Pergamon Press; London: 1965.
30. Homem MRP, Mascarenas NDA, Preza C. Biological Image Restoration in Optical-Sectioning Microscopy Using Prototype Image Constraints. *J. Real Time Imag.* 2002; 8:475–490.
31. Agard DA. Optical Sectioning Microscopy: Cellular Architecture in Three Dimensions. *Annu. Rev. Biophys. Bioeng.* 1984; 13:191–219. [PubMed: 6742801]
32. Faley S, Seale K, Hughey J, Schaffer DK, VanCompernelle S, McKinney B, Baudenbacher F, Unutmaz D, Wikswo JP. Microfluidic Platform for Real-Time Signaling Analysis of Multiple Single T Cells in Parallel. *Lab Chip.* 2008; 8:1700–1712. [PubMed: 18813394]
33. Goodey A, Lavigne JJ, Savoy SM, Rodriguez MD, Currey T, Tsao A, Simmons G, Wright J, Yoo SJ, Sohn Y, et al. Development of Multianalyte Sensor Arrays Composed of Chemically Derivatized Polymeric Microspheres Localized in Micromachined Cavities. *J. Am. Chem. Soc.* 2001; 123:2559–2570. [PubMed: 11456925]
34. Li SF, Floriano PN, Christodoulides N, Fozdar DY, Shao DB, Ali MF, Dharshan P, Mohanty S, Neikirk D, McDevitt JT, et al. Disposable Polydimethylsiloxane/Silicon Hybrid Chips for Protein Detection. *Biosens. Bioelectron.* 2005; 21:574–580. [PubMed: 16202870]
35. Smith, RA.; Giorgio, TD. Cytometry Part A. 2008. Quantitative Measurement of Multifunctional Quantum Dot Binding to Cellular Targets Using Flow Cytometry. DOI: 10.1002/cyto.a.20677
36. Soman CP, Giorgio TD. Quantum Dot Self-Assembly for Protein Detection With Sub-Picomolar Sensitivity. *Langmuir.* 2008; 24:4399–4404. [PubMed: 18335969]
37. Wikswo JP, Prokop A, Baudenbacher F, Cliffler D, Csukas B, Velkovsky M. Engineering Challenges of BioNEMS: The Integration of Microfluidics, and Micro- and Nanodevices, Models, and External Control for Systems Biology. *IEE Proc. Nanobiotechnol.* 2006; 153:81–101. [PubMed: 16948492]

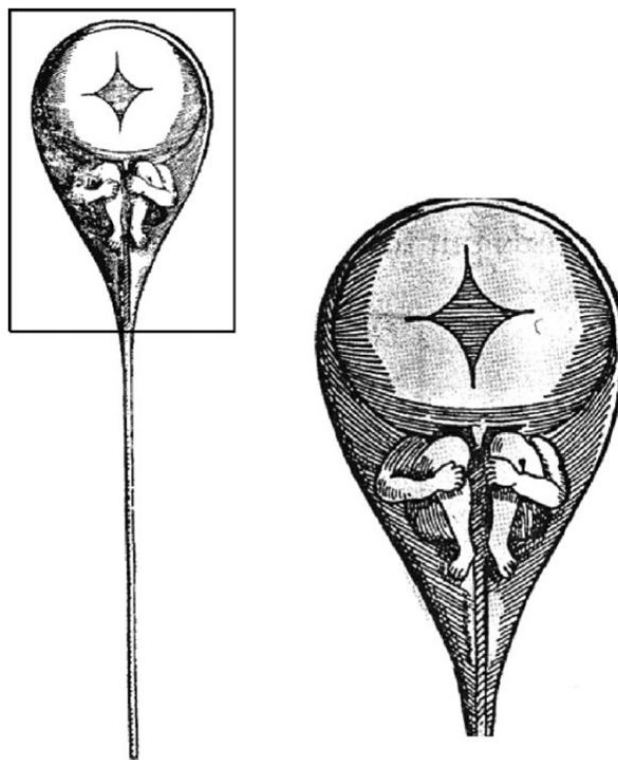


Figure 1. Drawing of a homunculus by Nicholas Hartsoecker, a famous misperception of sexual reproduction that would have been avoided with better microscope resolution. Public domain image from his *Essaie de dioptrique*, 1694.

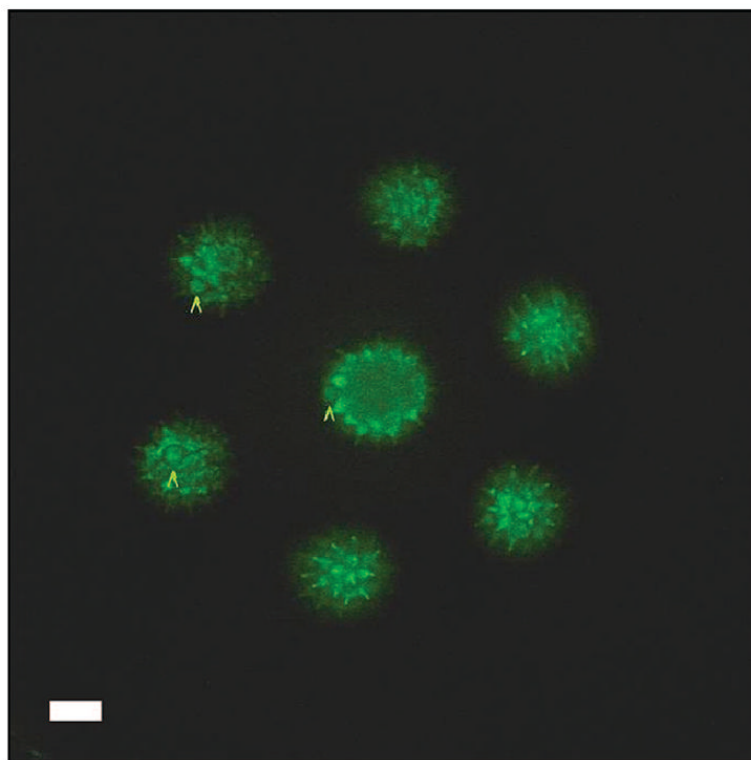


Figure 2. An image of a *Helianthus annuus* pollen grain collected with a seven-sided extroverted mirror. Caret indicates the same surface feature visible in three perspectives. The scale bar corresponds to 20 μm .

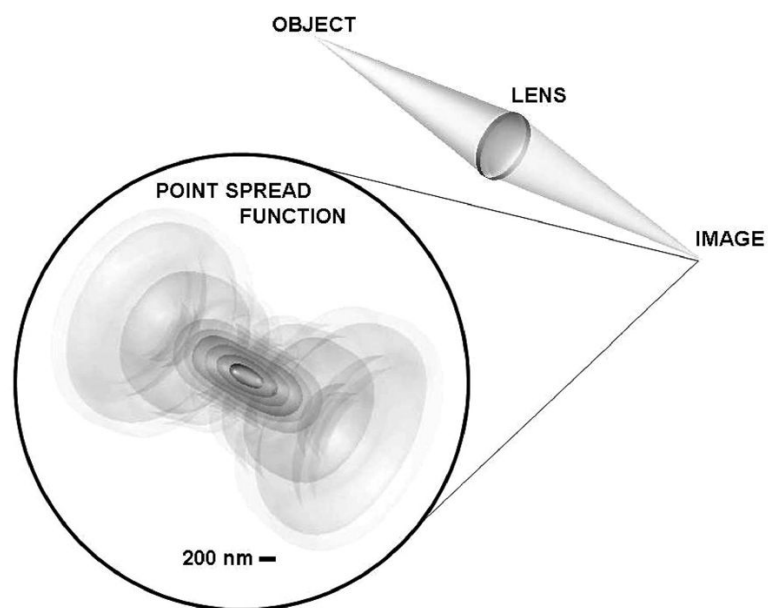


Figure 3. A point source as an object, a lens representing a microscope objective, the collection cone, and a 3D rendering of the isointensity surfaces in a theoretical point spread function (PSF) at the image (inset).

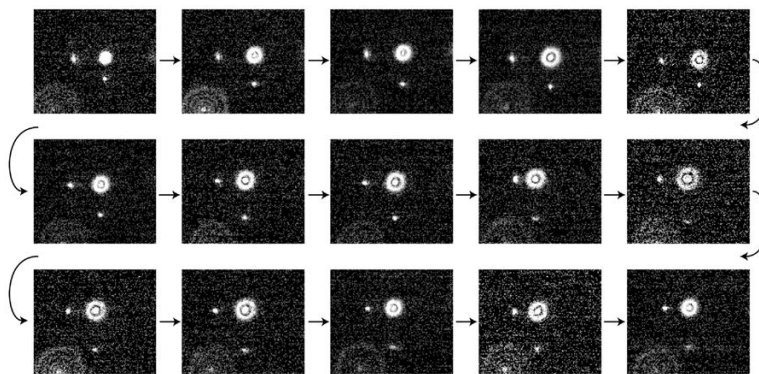


Figure 4. Higher-order maxima occur at radial positions that depend on the distance from the focal plane and appear in images as rings of light surrounding the point source. Images shown are a series from an orthogonal tracking movie of a 190 nm diameter particle in a water/glycerine solution and reproduced from McMahon *et al.*¹ Copyright 2009 American Chemical Society.

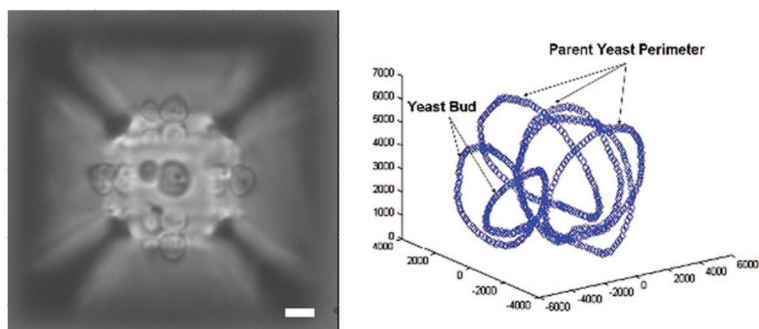


Figure 5. (Left) An arrested budding *Saccharomyces cerevisiae* cell in a MPW. (Right) A 3D affine reflection transformation reconstruction of the perimeters of the yeast and daughter bud. While the scale at right is uncalibrated, the scale bar on the left is approximately 7 μm .



Figure 6. Mirrored pyramidal well array etched on a silicon wafer (with a U.S. dime shown for scale). The pattern on the left contains 2940 wells of three different sizes. Image courtesy of John Russell.